Supplementary Information

SAS-6 coiled coil structure and interaction with SAS-5 suggests a regulatory mechanism in C. elegans centriole assembly

Renping Qiao, Gabriela Cabral, Molly M. Lettman, Alexander Dammermann and Gang Dong

Supplementary Methods

Isothermal titration calorimetry (ITC)

The purified SAS-6 CCD and the synthetic SAS-5 CTD (residues 390-404) or purified recombinant SAS-5 CTD fused to MBP were dialyzed overnight against a buffer containing 20 mM Tris-HCl (pH 8.0) and 50 mM NaCl. Protein and peptide concentrations were determined by ND-1000 spectrophotometer (PEQlab). ITC experiments were carried out at 25°C using a VP-ITC Microcal calorimeter (MicroCal, GE healthcare). The cell contained 1.4 ml of SAS-6 CCD dimer (10 μM, wild type or mutants), which was titrated with 29 injections × 10 μl of the SAS-5 CTD at a concentration of 105 μM. The ITC data were analyzed using the program Origin version 7.0 provided by MicroCal. One-site binding model was used to fit the integrated data to calculate the stoichiometry and binding constants.

For dilution ITC experiments, 300 μM of the SAS-6 CCD (dialyzed overnight) alone or in mixture with 450 μM of the SAS-5 CTD was injected into 1.4 ml of the same buffer in the temperature-controlled cell at 25°C. A total of 29 × 10 μl injections were carried out. Dissociation constants (K_d) were calculated by integrating and fitting the endothermic heat pulses to a dimer-tetramer dissociation model using Orign Version 7.0 (MicroCal).

Static light scattering (SLS)

The SLS studies were carried out on an instrument from the Wyatt Technology Corp. The liquid chromatography equipment consists of a HPLC system (Agilent Technologies) connected in series with a triple-angle laser light scattering detector (miniDAWN TREOS), a

UV detector at 280 nm (Agilent technologies) and a refractive index detector (RI-101, Shodex). 100 µl of protein samples (4 mg/ml for the SAS-6 CCD and 6 mg/ml for the MBP-SAS-5 CTD) were eluted from a Superdex 200 10/300 GL column (GE healthcare) at a flow rate of 0.5 ml per min. Data analysis was carried out using the Astra software (Wyatt technology).

C. elegans strains and culture conditions

To generate the SAS-6:GFP strain, the *sas-6* genomic locus, including 1.8 kb upstream and 0.5 kb downstream regulatory sequences and a 300bp re-encoded region of the last exon for RNAi resistance (Dammermann et al., 2008) was cloned into the Chromosome II integration vector pCFJ151 together with an in-frame C-terminal GFP tag. Mutant forms were generated by site directed mutagenesis on a small fragment of the coding sequence which was then reintroduced into the wild-type construct by subcloning. All constructs were verified by DNA sequencing. Transgenesis was performed in the EG6249 strain which contains a transposon insertion on Chromosome II (Frokjaer-Jensen et al., 2008). Proper integration was confirmed by single-worm PCR with primers spanning the homology arms. For recruitment analysis, L4 hermaphrodites were mated to males expressing mCherry:SAS-4 (Dammermann et al., 2008). All strains used are listed in Supplemental Table I. Strains were maintained at 23 C, except when performing RNA-mediated interference.

RNA-mediated interference

Double-stranded RNAs were prepared from N2 genomic DNA using the primer sets listed in Supplemental Table II (Dammermann et al., 2008) and injected into L4 hermaphrodies. All RNAs were at concentrations of >1mg/ml. Standard RNAi conditions of 48h at 16 C were used to ensure full depletion.

Image acquisition

Embryos were filmed without compression (Monen et al., 2005) on a Yokogawa CSU X1-A1 spinning disk confocal mounted on a Zeiss Axio Observer Z1 inverted microscope equipped with a 63 × 1.4NA Plan Apochromat lens (Zeiss), Visitron Systems Laser module 1875 with 100 mW 488 nm and 561 nm solid-state lasers, laser merge and AOTF-100 unit and a Photomoetrics CoolSNAP-HQ2 cooled CCD camera. Acquisition parameters, shutters and focus were controlled by VisiView software (Visitron Systems). Embryos were monitored by DIC microscopy from pronuclear migration until the end of the second mitotic division. GFP(/mCherry) z-series with a step size of 0.5 μm were performed in the first and second mitosis to examine GFP:SAS-6 localization/recruitment. For these, exposure times of 500 ms with 4×4 binning at full laser power were used to collect sufficient signal. Image stacks were imported into MetaMorph for post-acquisition processing. Panels are single-plane or maximum intensity projections of multiple planes depending on centrosome positioning within the embryo. Images are auto-scaled for best presentation unless otherwise noted.

Supplementary Tables

Supplementary Table I: *C. elegans* strains used in this study.

Strain	**Genotype**
EG6249	ttTi5605 II; unc-119(ed3) III
OD467	ltSi40[pOD1227; Psas-6::SAS-6reencoded::GFP; Cb-unc-119(+)]II; unc-119(ed3)III
DAM430	vieSi34[pAD509; Psas-6::SAS-6reencoded-mA::GFP; Cb-unc-119(+)]II; unc-119(ed3)III
DAM431	vieSi35[pAD511; Psas-6::SAS-6reencoded-mD::GFP; Cb-unc-119(+)]II; unc-119(ed3)III
DAM260	ltIs64 [pOD333; Ppie-1::mCherry-TEV-Stag::sas-4 genomic; unc-119(+)]I

Supplementary Table II: dsRNAs used in this study.

dsRNA	**µg/µl**	**Oligo #1**	**Oligo #2**
sas-5	4.5	AATTAACCCTCACTAAAGGAG GACAAAACCCCCAGTACC	TAATACGACTCACTATAGGAG AAGCGAGTCCGTTGTCAT
sas-6	5.6	AATTAACCCTCACTAAAGGTA TGGAGCTAATTTGAACTCGGT TA	TAATACGACTCACTATAGGAG CAGAGTTTTATTTTCAAGTAA AGGA

Supplementary Figures

Qiao et al, Fig. S1

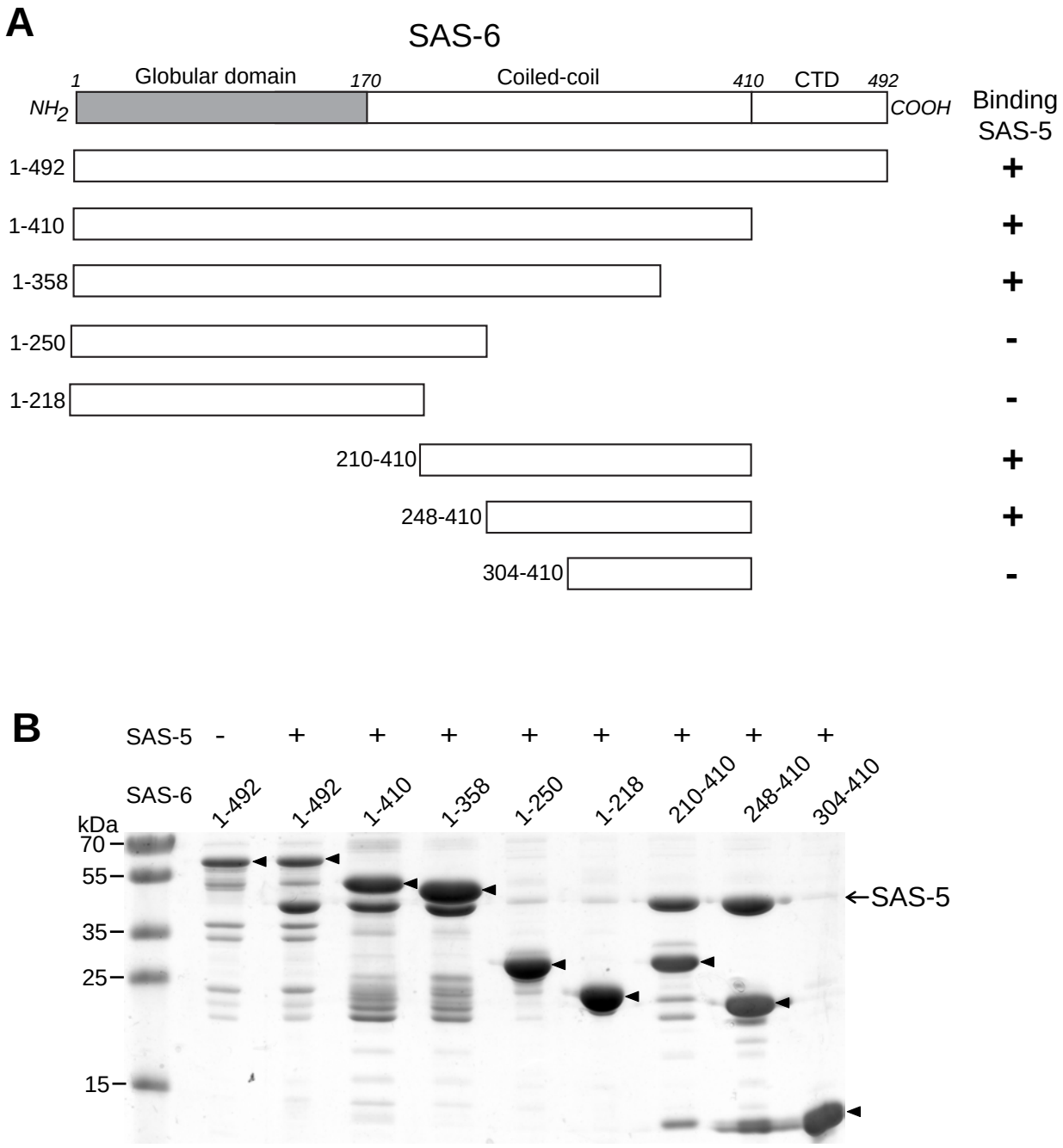

Supplementary Figure S1. The SAS-5 CTD binds specifically to the central part of the SAS-6 coiled coil. (**A**) Truncation constructs of SAS-6 used for *in vitro* binding assays with the SAS-5 CTD (residues 390-404). Numbers in front of the constructs indicate amino acid ranges. The right column shows the summary of the binding results in (B). (**B**) *In vitro* pull-down results of MBP-tagged SAS-5 CTD using Ni-NTA bound SAS-6 of various lengths as the baits. Arrowheads indicate SAS-6 proteins.

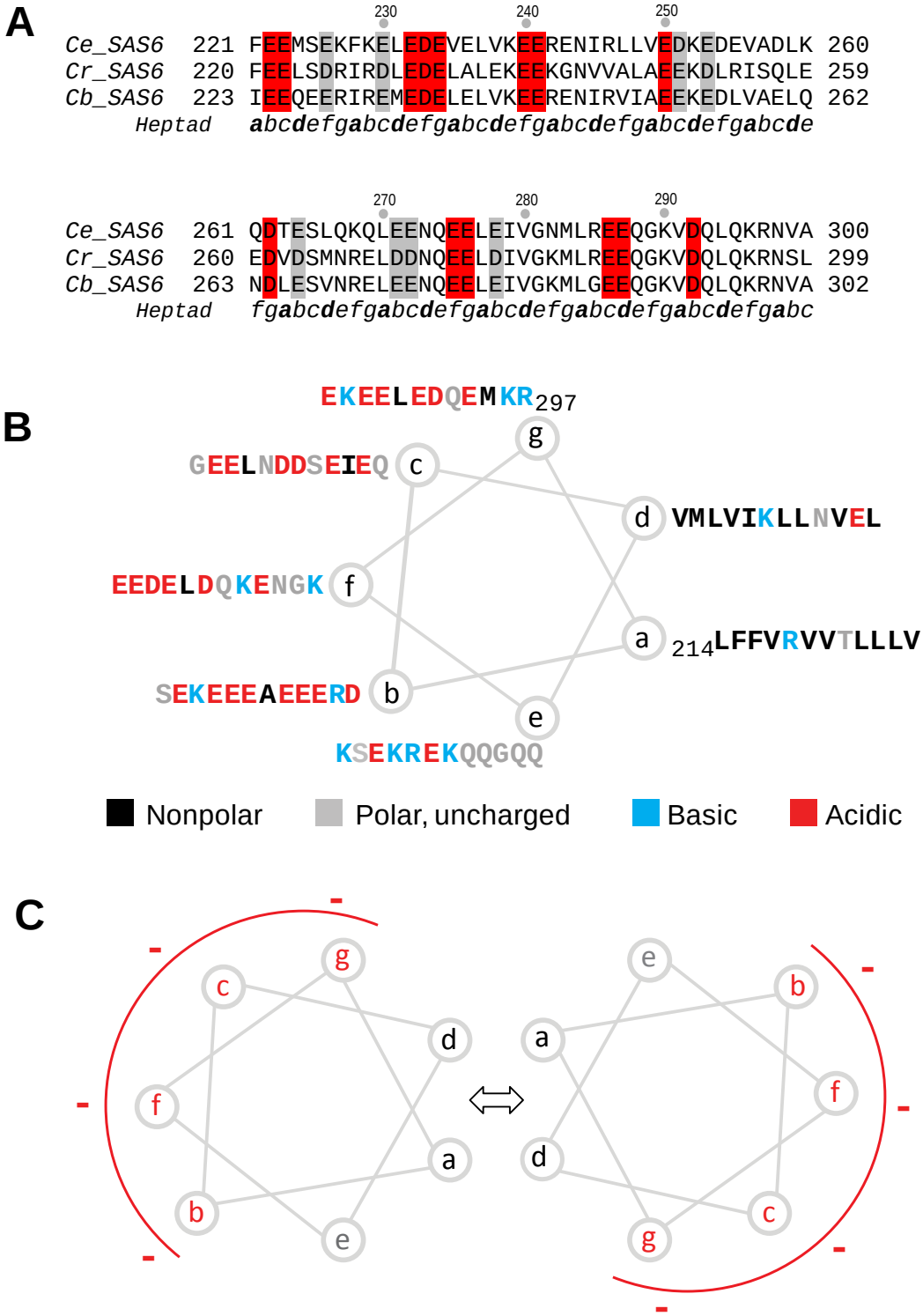

Supplementary Figure S2. The "neck" region of the *C. elegans* SAS-6 coiled coil (residues 221-300) is predominantly negatively charged. (**A**) Sequence alignment of the N-terminal part of the SAS-6 coiled coil from three *Caenorhabditis* species. *Ce, Caenorhabditis elegans; Cr, C. remanei; Cb, C. briggsae*. Identical negatively-charged residues (D or E) are shaded in red; conserved ones are highlighted in grey. The heptad registers of the residues are shown beneath the aligned sequences. Registers of residues 250-300 are extracted from the crystal structure and those for the preceding residues are derived from coiled-coil predictions (http://www.ch.embnet.org/software/COILS_form.html). (**B**) Helical wheel diagram looking down the helix axis from the N- to the C-terminus of the SAS-6 coiled coil (residues 221-300). Heptad positions are labeled *a* to *g*. Positions *a* and *d* are occupied predominantly by nonpolar hydrophobic residues whereas other positions are mostly polar or charged residues. (**C**) Helical wheel representation of the parallel homodimer of the SAS-6 coiled coil (residues 221-300). Inter-helical hydrophobic interactions are denoted as a wide arrow. Negatively-charged surfaces formed by residues at positions *b, c, f,* and *g* are shown by red curves.

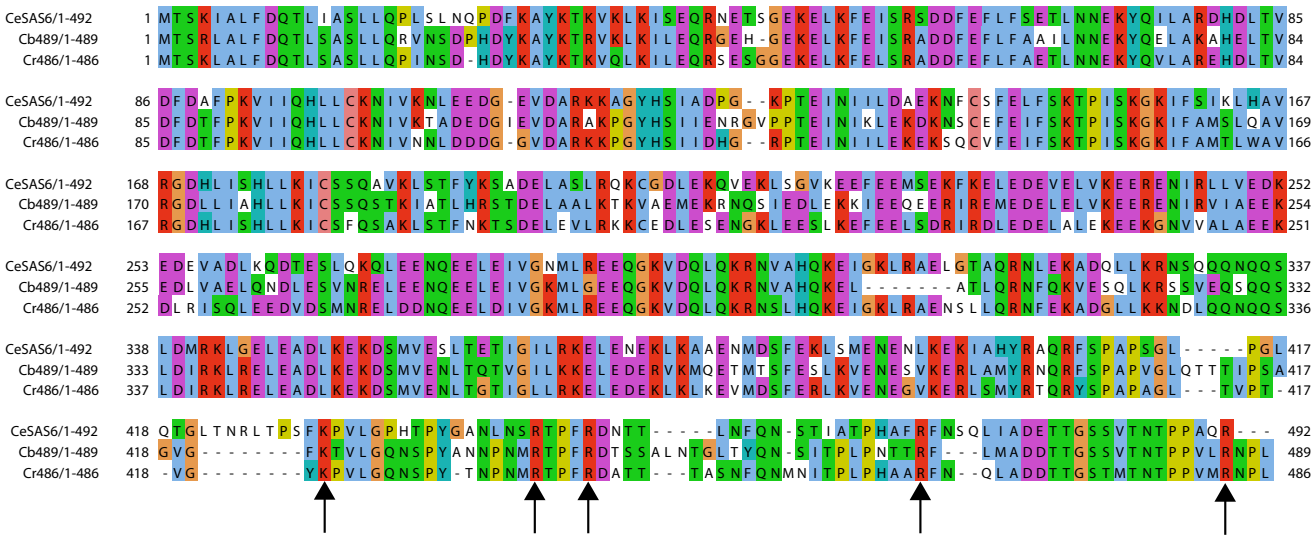

Supplementary Figure S3. Sequence alignment of SAS-6 proteins from three *Caenorhabditis* species. *Ce, Caenorhabditis elegans; Cr, C. remanei; Cb, C. briggsae.* The five conserved positive residues in the C-terminal domain are indicated by arrows.

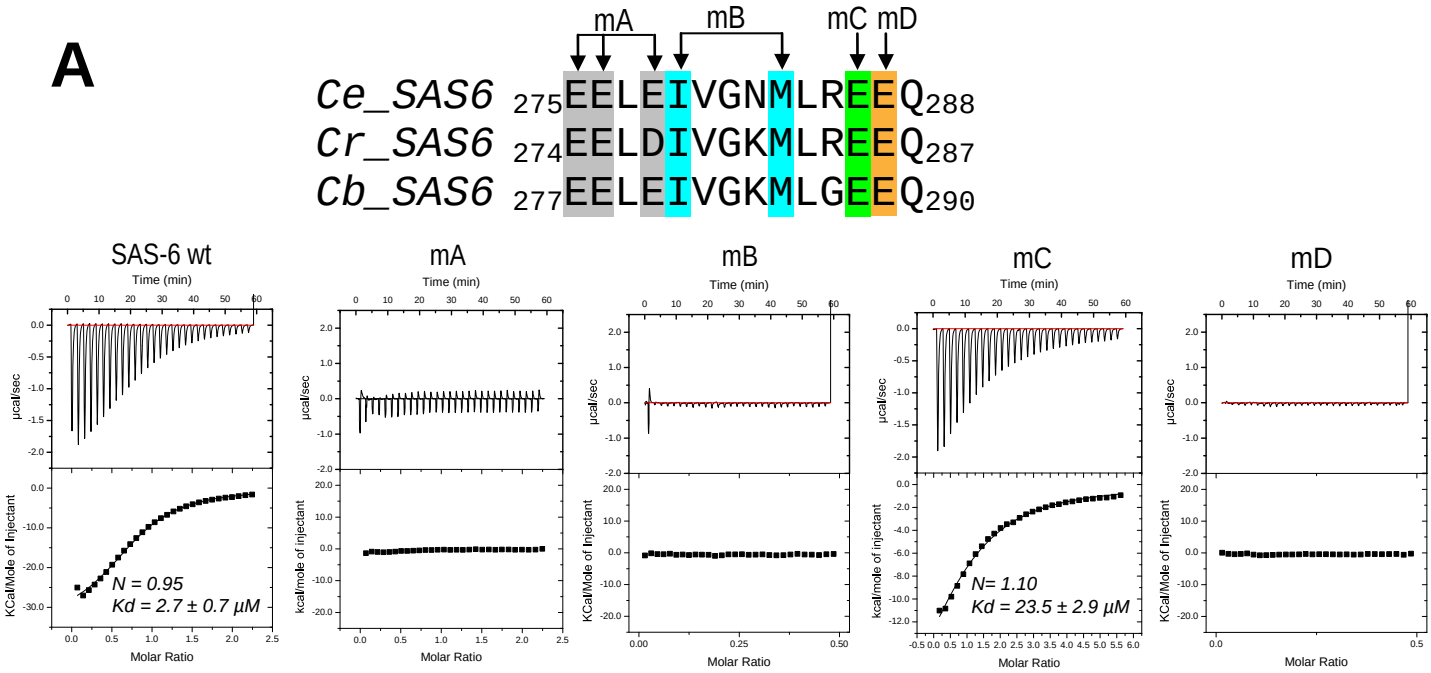

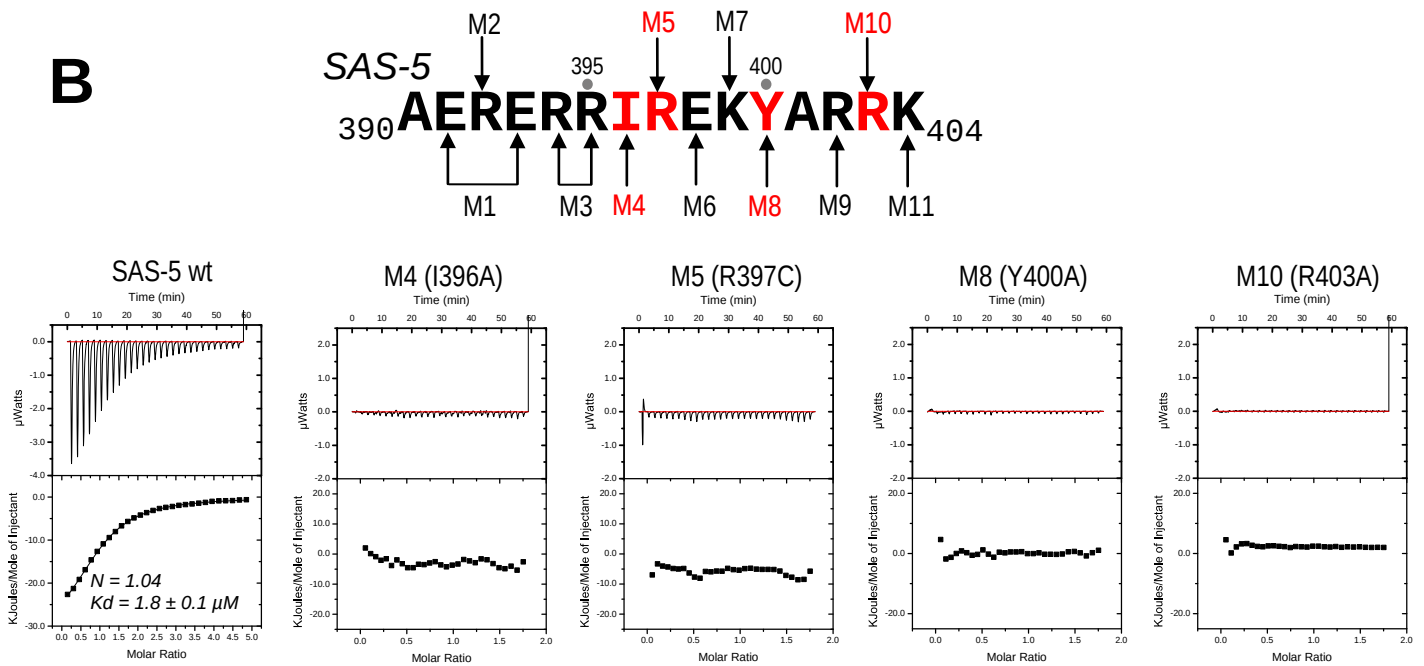

Supplementary Figure S4. ITC titrations of mutations of SAS-6 or SAS-5. (A) ITC titrations and fit curves for wild-type (wt) and four mutations of SAS-6 interacting with the SAS-5 CTD. Mutations mA, mB, and mD completely abolished the interaction between SAS-6 and SAS-5, whereas the mutation mC only mildly reduced the binding affinity. (**B**) ITC titrations and fit curves for wild-type (wt) and four mutations of the SAS-5 CTD interacting with the SAS-6 CCD. No measurable Kd was detected for all these mutations.

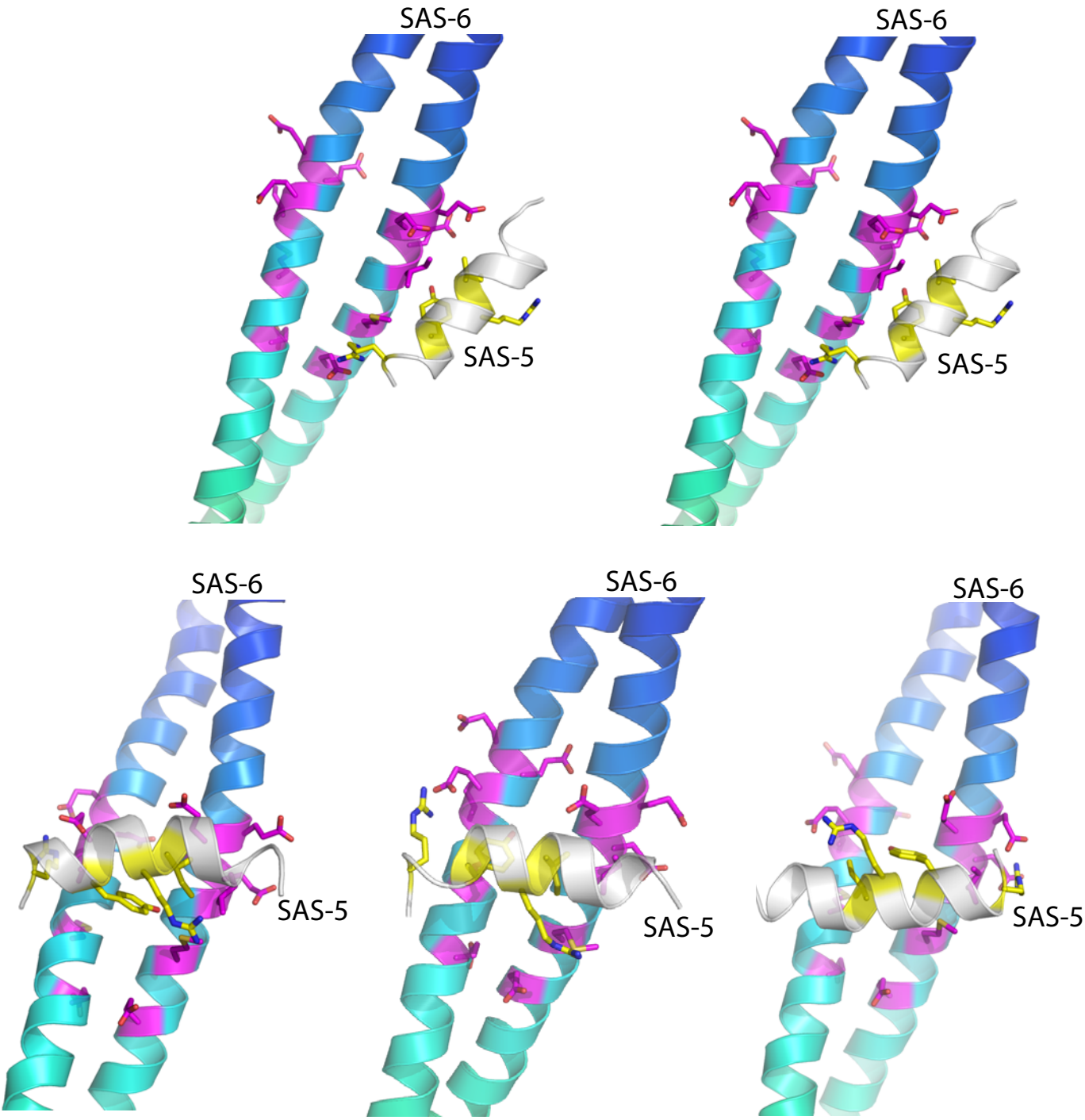

Supplementary Figure S5. Five alternative interacting models of SAS-5 and SAS-6 predicted by the ClusPro 2.0 docking server (http://cluspro.bu.edu/). Side chains of the residues involved in the interaction, which were mapped by our mutagenesis studies, are shown in sticks with color schemes of magenta in SAS-6 and yellow in SAS-5.

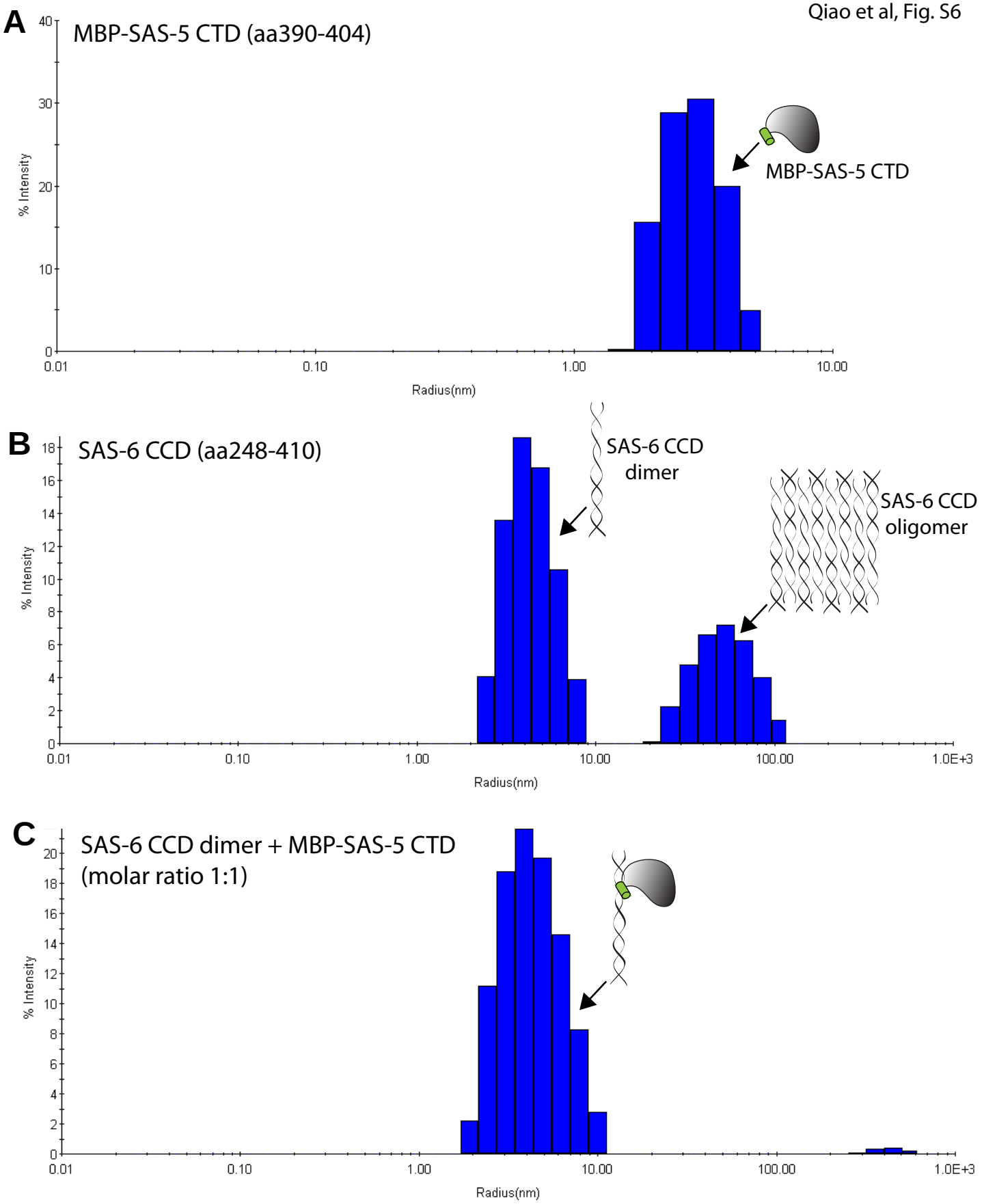

Supplementary Figure S6. DLS-determined size distributions of SAS-5 CTD, SAS-6 CCD, and their complex. (**A**) MBP-SAS-5 CTD (residues 390-404, 20μM) shows a monodisperse signal. (**B**) SAS-6 CCD (residues 248-410, 15μM) shows two peaks. The majority of the mass (~99.9%) is in the 4-nm peak, which is the dimer of the SAS-6 CCD, whereas the 50-nm peak only represents 0.1% of the total mass and is likely the oligomeric form of the CCD, which, without the obstruction of the head group, could form a large assembly. (**C**) Mixture of the SAS-6 CCD dimer and the SAS-5 CTD (1:1, 15μM each) shows a single peak, which suggests that binding of SAS-5 prevents the oligomerization of the SAS-6 CCD.

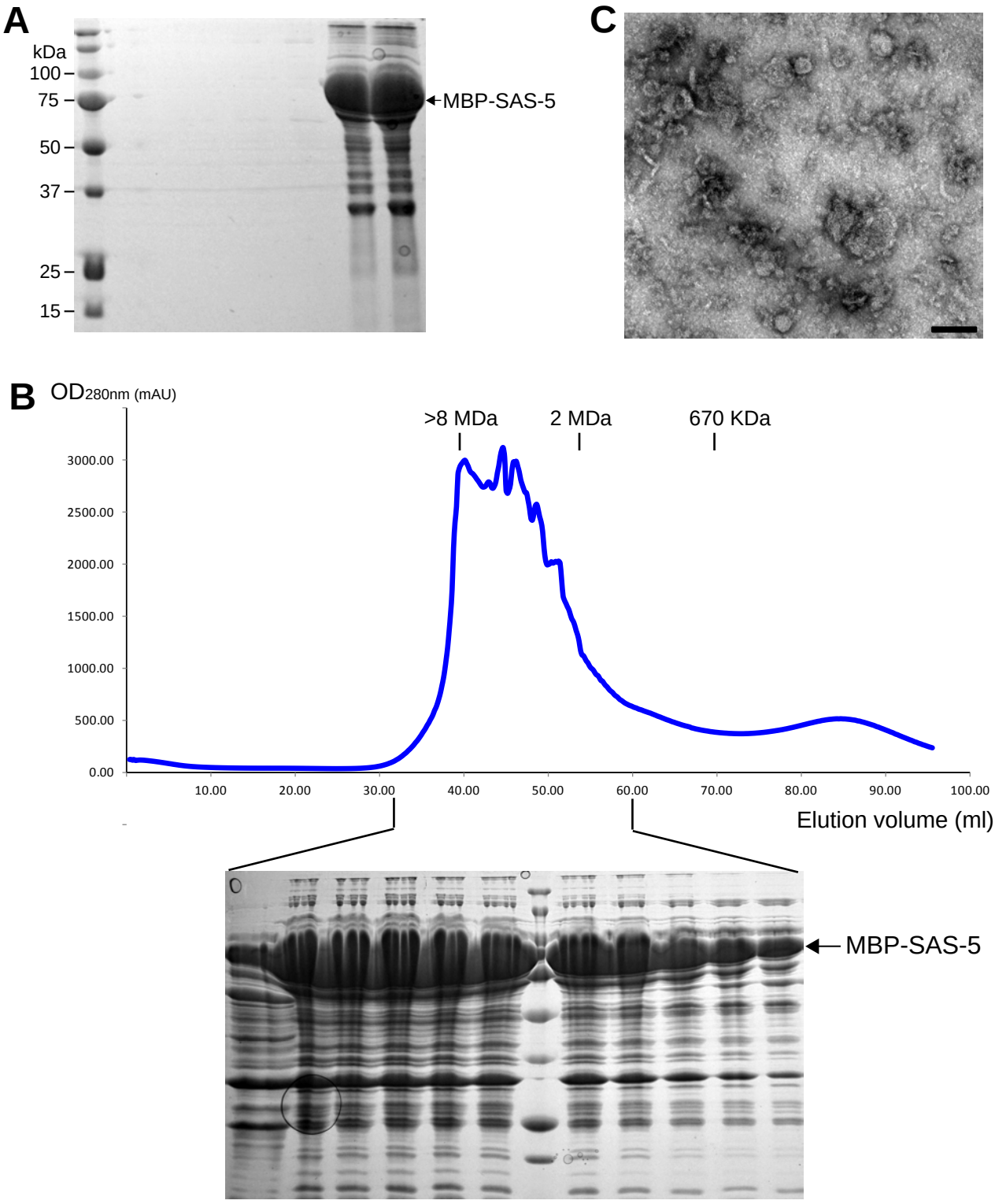

Supplementary Figure S7. SAS-5 on its own forms aggregates. (**A**) Partially purified recombinant MBP-tagged SAS-5 using ammonium sulfate precipitation. (**B**) Size exclusion chromatography of MBP-SAS-5 on a Superdex-400 (16/60) column. SAS-5 was eluted at factions near the void volume of the column. (**C**) Negative staining electron micrograph of MBP-SAS-5. Large irregular aggregates can be seen. Scale bar, 100 nm.

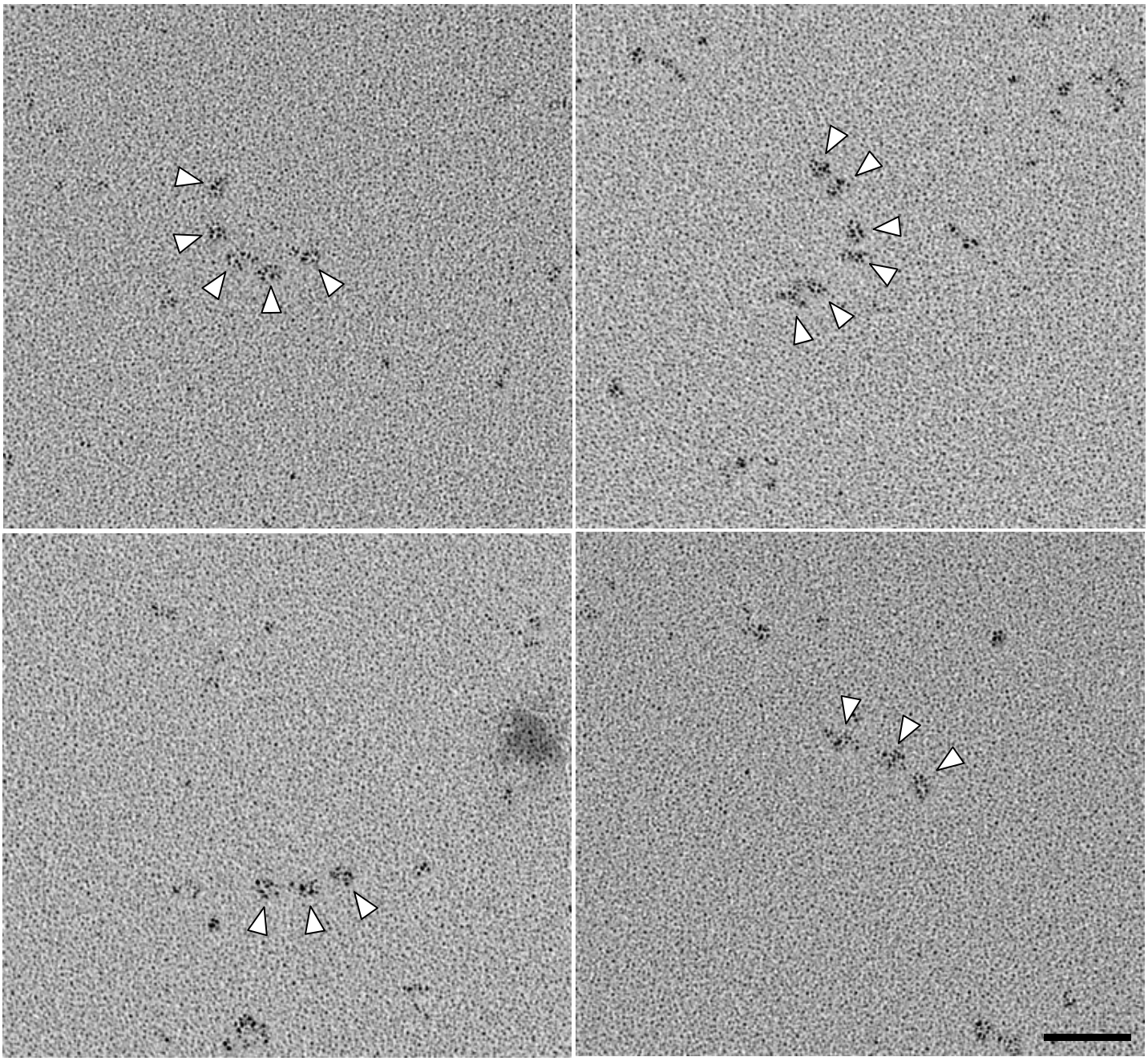

Supplementary Figure S8. Large fields of rotary metal shadowing images of the SAS-5/SAS-6 complex. Four large-field images are shown to indicate that the arc-like structures are repeatedly formed on a rather clean background. Therefore, the structures are unlikely to be artifacts. Arrowheads indicate the globular structures arranged in a semicircle or arc-like manner. Scale bar, 50 nm.

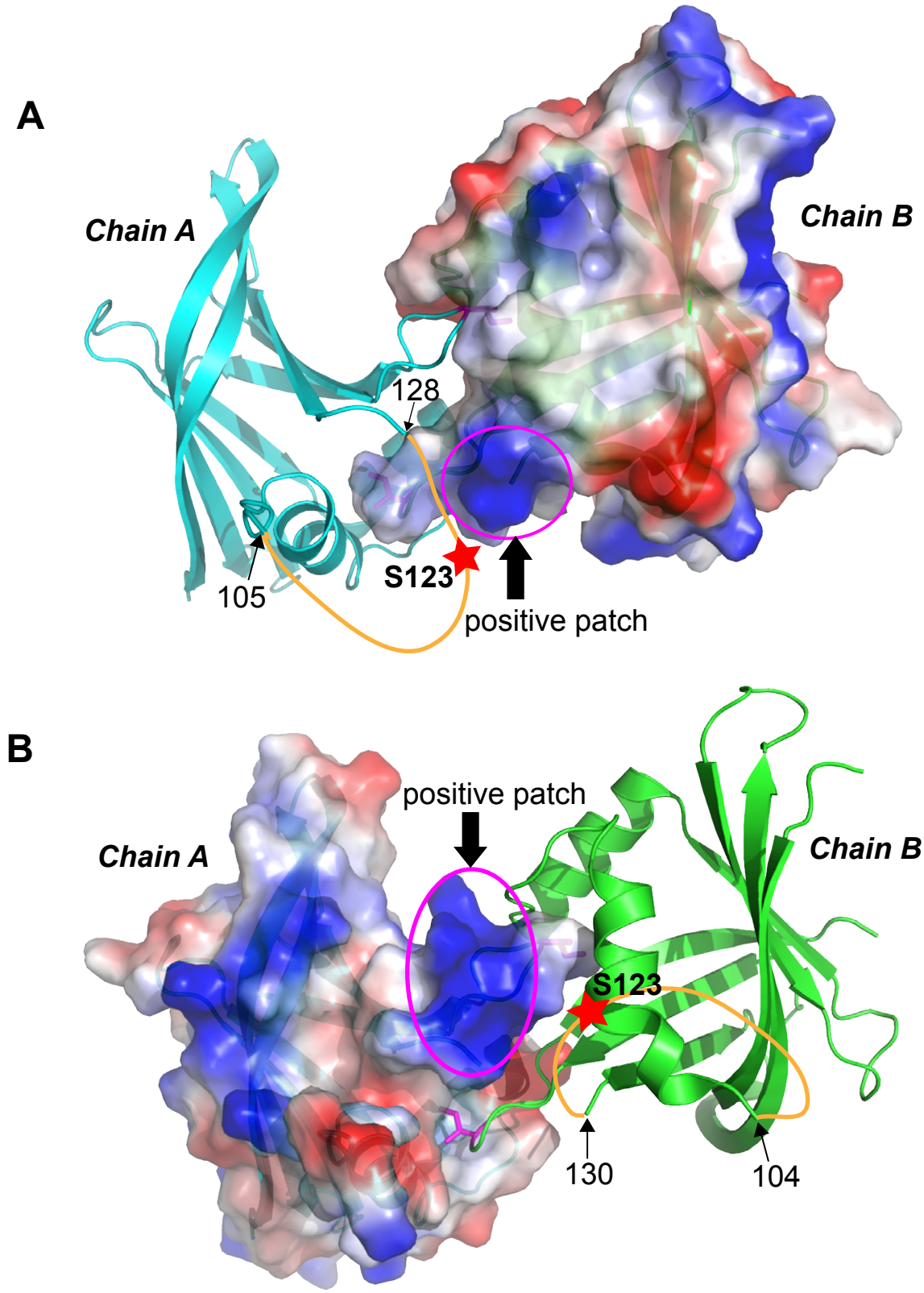

Supplementary Figure S9. ZYG-1 mediated phosphorylation of S123 on SAS-6 may strengthen the interaction between the head groups of SAS-6. The residue S123 is located in the flexible loop (gold) adjacent to the dimerization interface. It is spatially close to a positively charged surface patch (magenta circles) on the neighboring molecule. It is conceivable that phosphorylation of S123 by ZYG-1 may stabilize the head group interaction of SAS-6 by providing an electrostatic interaction between the phospho-group and the positive surface patch on the opposite molecule. (**A**) View of the spatial orientation of S123 on chain A and a positive patch on chain B. (**B**) The same view as in (A) but showing the spatial orientation of S123 on chain B and a positive patch on chain A.

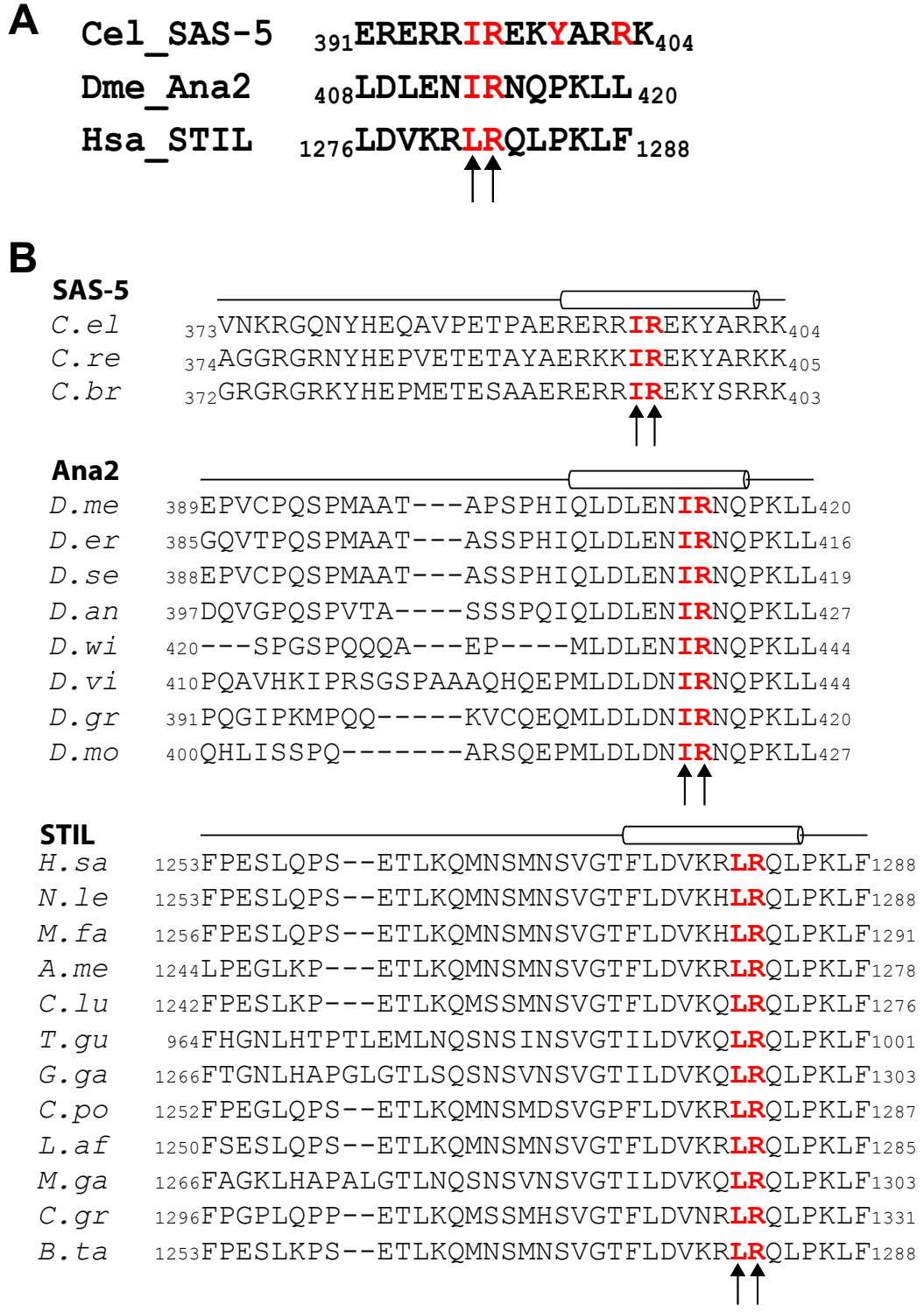

Supplementary Figure S10. Comparison of the TIM motifs at the extreme C-terminus of SAS-5, Ana2 and STIL. (**A**) Ana2 and STIL contain two of the four residues in the SAS-5 CTD that are essential for SAS-6 interaction. *Cel, Caenorhabditis elegans; Has, Homo sapiens; Dme, Drosophila melanogaster.* (**B**) The TIM motifs are all predicted to contain an α-helix, which is preceded by a disordered loop. Two of the four key residues in the SAS-5 CTD essential for SAS-6 interaction are also conserved in flies and vertebrates (arrows).